



HAL
open science

Rat hepatocytes express functional P2X receptors.

Emmanuel Gonzales, Sylvie Prigent, Aurélie Abou-Lovergne, Sylviane Boucherie, Thierry Tordjmann, Emmanuel Jacquemin, Laurent Combettes

► **To cite this version:**

Emmanuel Gonzales, Sylvie Prigent, Aurélie Abou-Lovergne, Sylviane Boucherie, Thierry Tordjmann, et al.. Rat hepatocytes express functional P2X receptors.: Rat hepatocytes express functional P2X receptors. FEBS Letters, 2007, 581 (17), pp.3260-6. 10.1016/j.febslet.2007.06.016 . inserm-00276672

HAL Id: inserm-00276672

<https://inserm.hal.science/inserm-00276672>

Submitted on 30 Apr 2008

HAL is a multi-disciplinary open access archive for the deposit and dissemination of scientific research documents, whether they are published or not. The documents may come from teaching and research institutions in France or abroad, or from public or private research centers.

L'archive ouverte pluridisciplinaire **HAL**, est destinée au dépôt et à la diffusion de documents scientifiques de niveau recherche, publiés ou non, émanant des établissements d'enseignement et de recherche français ou étrangers, des laboratoires publics ou privés.

**Rat hepatocytes express functional P2X receptors**

Emmanuel Gonzales^{1,2,*}, Sylvie Prigent¹, Aurélie Abou-Lovergne¹, Sylviane Boucherie¹,
Thierry Tordjmann¹, Emmanuel Jacquemin², Laurent Combettes¹

¹ INSERM; Université Paris-Sud, UMR-S757, Bâtiment 443, 15 rue Georges Clémenceau, 91405 Orsay cedex, France.

² CHU Bicêtre Assistance publique - Hôpitaux de Paris, Hépatologie Pédiatrique, 94275 Le Kremlin Bicêtre Cedex, France

* Corresponding author. Tel.: +33 1 69 15 63 96; fax: +33 1 69 15 58 93.

E-mail address: emmanuel.gonzales@gmail.com (Emmanuel Gonzales).

Keywords: Purinergic receptors, ATP, Blebbing, Hepatocytes, Liver, Nucleotide receptor.

Abbreviations: YO-PRO-1, 4-[(3-methyl-2(3H)-benzoxazolylidene)methyl]-1-[3-(triethylammonio)propyl]diiodide; BzATP, 2'- and 3'-O-(4-benzoylbenzoyl)-ATP; oATP, oxidised ATP.

1. Introduction

Extracellular nucleotides are emerging as ubiquitous mediators of cell-cell communication in most tissues [1], and as potent stimuli for the release of bioactive factors from many different cell types [2]. Extracellular ATP is present in bile and hepatic venous blood in the liver, albeit at low concentrations. It is also present in the supernatant of cultured cells of hepatic origin [see 3 for review]. ATP may also be released in response to various stimuli, such as mechanical stimulation, increase in cell volume [4-5]. Once in the pericellular environment, ATP modulates many important hepatic functions, such as gluconeogenesis, protein synthesis and bile secretion [6-7], via specific P2 receptors. There are several types of P2 receptors: ligand-gated cationic channels or P2X receptors, and G protein-coupled P2Y receptors. In the liver, P2Y receptors are expressed by all cell types [1, 6, 8-9] and are well characterized [10]. However, it has been suggested that activation of a P2Z receptor, now known as P2X7 [11], is involved in ATP-induced cytotoxicity in hepatocytes [12]. Furthermore, ATP has been shown to activate a cation-selective current in isolated guinea pig hepatocytes even in the absence of a P2Y response [13]. The aim of the present study was to investigate the presence of functional P2X receptors in rat hepatocytes.

2. Materials and Methods

Materials

Williams' medium E was obtained from Life Technology (Invitrogen, France), and collagenase A, from Boehringer (Roche Diagnostics, France). P2X receptor primers for reverse transcriptase-polymerase chain reaction (RT-PCR) and other chemicals were purchased from Sigma (Sigma-Aldrich, France).

Hepatocyte preparation

Experiments were conducted according to EC directives for animal experimentation (decree 2001-131; Official Journal 06/02/01). Hepatocytes were prepared from fed Wistar rats as previously described [14]. Isolated rat hepatocytes were maintained (2×10^6 cells/mL) at room temperature in Williams' medium E supplemented with 10% fetal calf serum, penicillin (200,000 U/mL) and streptomycin (100 mg/mL). Cell viability, assessed by trypan blue exclusion, remained > 96%, for 4 to 5h.

In some experiments, liposomal clodronate suspension (4 ml/kg) was injected intravenously into the rats 48h before inclusion in the experiments, to eliminate Kupffer cells [15]. Monoclonal antibodies against ED2 (Serotec, Oxford, UK), a marker of tissue macrophages [16], were used in immunofluorescence assays to assess the effectiveness of liposomal clodronate treatment (Supplementary Fig. 1S).

RT-PCR

Total RNA was extracted from freshly isolated hepatocytes, whole heart and brain preparations, using Trireagent[®] (SIGMA), according to the manufacturer's recommendations. Reverse-transcribed mRNA (cDNA) was amplified by PCR in the presence of independent

sense and antisense primers. Primers and PCR conditions are described in the supplementary data (Tab. 1S). Amplification products were separated by gel electrophoresis (2% agarose) and visualised by ethidium bromide staining.

Western blotting

Proteins (30 to 50 μ g) in crude membrane preparations from hepatocytes were solubilised, resolved by 7.5% SDS-polyacrylamide gel electrophoresis and transferred to a nitrocellulose membrane (Hybond ECL, Amersham). The positive controls for P2X4 and P2X7 receptors were respectively rat salivary gland membranes [17] and c-myc tagged mouse P2X7-transfected HEK cells lysates (kindly provided by Dr K. Benihoud). Immunoblotting was performed with anti-P2X4 or anti-P2X7 polyclonal antibodies (Alomone) and the appropriate peroxidase-conjugated secondary antibodies (Pierce). Peroxidase activity was detected with an enhanced chemiluminescence kit (Amersham Biosciences Europe).

Immunocytochemistry. Isolated hepatocytes were seeded on glass slides, washed with PBS, and fixed (ethanol 30min at 4°C, then acetone 1min). Cells were incubated for 1h with the anti-P2X4 or anti-P2X7 antibody (1:200 in PBS), then washed in PBS and incubated with the appropriate Alexa-conjugated secondary antibodies (Molecular Probes). After mounting, cells were examined with an Axioskop fluorescence microscope (Zeiss, Germany), or with a confocal microscope (Nikon EZC1) equipped with a x63 plan-apochromatic oil immersion objective (NA=1.4). Images were processed using Image J software.

Determination of calcium changes in hepatocytes

Hepatocytes were plated onto glass coverslips coated with type I collagen and loaded with 3 μ M Fura2-AM in modified Williams' medium, for 40min, (37°C, 5%CO₂). After washing

the coverslips were transferred into a perfusion chamber placed on the stage of a Zeiss (Axiovert 35) inverted microscope. Calcium imaging was performed as described previously [14]. Fluorescence images were collected by a CCD camera (Princeton, USA), digitized and integrated in real time by an image processor (Metafluor, Princeton, USA).

YO-PRO-1 uptake. After isolation, hepatocytes were stored at room temperature in Eagle medium supplemented with amino acids, vitamins and gelatin, and gassed with O₂/CO₂ (19:1) at pH 7.4, until use, as described previously [14]. Cells were centrifuged, washed and resuspended in 1μM YO-PRO-1 (Molecular Probes) in saline (mM : 116 NaCl, 5.4 KCl, 1.8 CaCl₂, 0.8 MgCl₂, 0.96 NaH₂PO₄, 5 NaHCO₃, 20 HEPES, and 1g/L glucose, pH 7.4). Cell suspensions were transferred either to a spectrofluorometer cuvette (5x10⁵cells/mL) and stirred with a magnetic bar at 37°C (Varian) or incubated for 30min at 37°C in a 96-well flat-bottomed microtiter plate (5x10⁴cells/well), then fluorescence was monitored in a 96-well plate fluorometer (Victor 3, Wallac & Perkin Elmer). In each case, fluorescence was measured at the optimum wavelengths for YO-PRO-1, 485nm (λ_{ex}) and 530nm (λ_{em}). Data were collected as arbitrary fluorescence units, and increases in fluorescence induced by agents were expressed as a percentage of basal fluorescence ($\Delta F/F$ %). In some experiments, Triton (0.01%) was added to measure YO-PRO-1 maximum fluorescence after cell permeabilization. Statistical analyses were performed with Prism version 4 (GraphPad Software, USA), using Student's t test, with *P* values <0.05 considered significant.

3. Results and Discussion

Detection of P2X receptor subunits in hepatocytes.

cDNAs generated from six independent rat hepatocyte preparations were probed by RT-PCR, using pairs of oligonucleotides specific for P2X1-7 amplification. As a positive control, amplified products of the appropriate sizes for P2X1, P2X4 and P2X5 were detected following PCR with rat heart cDNA and products corresponding to P2X2, P2X3, P2X6 and P2X7 were detected following PCR with rat brain cDNA [18]. P2X4, and P2X7 mRNAs were present in all hepatocyte preparations (Fig. 1) in which we did not detect mRNAs for P2X1, P2X2, P2X3, and P2X5. P2X6 mRNA gave a weak signal in one preparation.

P2X4 and P2X7 receptors are expressed at high levels in macrophages [1, 19]. The resident liver macrophages, Kupffer cells, have recently been shown to express P2X4 and P2X6 receptors [20]. Although the method of hepatocyte isolation used in this study yielded a cellular population containing 99% hepatocytes [21], possible contamination with Kupffer cells has to be considered. We therefore isolated hepatocytes from rats treated with clodronate liposomes, which selectively eliminates macrophages (Supplementary Fig. 1S) and found that P2X4, and P2X7 mRNAs were similarly detected in control and treated rats (Fig. 2A).

Identification of P2X4 and P2X7 receptor proteins in hepatocytes.

We found both P2X4 and P2X7 receptor proteins in hepatocytes isolated from control or clodronate-treated rats by Western blot analysis with isoform-specific antibodies (Fig. 2B). As shown in other cell types [22], although the predicted molecular mass of P2X4 is about 46kDa, protein bands of ~65kDa were recognised for P2X4 both in rat salivary gland membranes and in hepatocyte membranes isolated from the livers of control or clodronate-

treated rats. For Western blot analysis of P2X7 expression, hepatocyte lysates from the livers of control or clodronate-treated rats were run in parallel with sample lysates from wild-type or c-myc tagged mouse P2X7 HEK transfected cells. As in other cell types [23], the antibody recognised a distinct protein band at ~70kDa. The protein detected in transfected HEK cells lysates was slightly larger than the rat P2X7 receptor, due to both the presence of a c-myc tag and interspecies difference [18]. In each case, immunoreactivity was prevented by prior incubation of the antibody with its cognate peptide (data not shown).

The molecular mass of about 70kDa for each receptor subunit is consistent with published data describing P2X receptors as highly glycosylated proteins [18]. The presence of alternatively spliced P2X receptor isoforms, together with post-translational modifications, gives rise to potentially large variations in the size of the detected proteins [18, 24].

Immunolocalization of P2X4 and P2X7 in hepatocytes.

We next investigated the distribution of P2X4 and P2X7 immunoreactivity in isolated hepatocytes. Staining with anti-P2X4 antibody was patchy, and located both at the plasma membrane and throughout the cytoplasm (Fig. 3A and Supplementary Mov. 1S). Interestingly, in almost all the hepatocyte doublets analyzed, strong labeling was observed near the bile canaliculus area (Fig. 3A inset). This particular distribution is consistent with the already reported role of P2X4 receptor in bile secretion [25]. In contrast, anti-P2X7 staining was not preferentially localized in the area of the bile canaliculus. Instead, a patchy distribution was observed concentrated along the plasma membrane (Fig. 3B and inset).

Functionality of P2X receptors in hepatocytes.

If ATP is added onto cells for a short time, the P2X4 and P2X7 receptors operate as cation-selective channels [18]. This is particularly true for P2X4, which has a relatively high Ca^{2+}

permeability. However, assessments of the increase in Ca^{2+} concentration in hepatocytes for evaluations of the functionality of P2X receptors may be complicated by the presence of G protein-coupled P2Y receptors, which induce an increase in Ca^{2+} concentration through an inositol 1,4,5-trisphosphate (InsP3) production [10]. In effect, as shown in Fig. 4, addition of low concentration of BzATP (30 μM), the P2X-preferring agonist, induced Ca^{2+} oscillation similar to those induced by InsP3 dependant agonists [10]. Moreover, BzATP-induced Ca^{2+} oscillations were not significantly modified by prior incubation of hepatocytes for 2h with oATP (300 μM), an antagonist with some specificity for the P2X7 receptor [11, 18, 26] (Fig. 4B). In the same way, as with InsP3 dependent agonists, an increase in the concentration of BzATP (300 μM) induced a sustained Ca^{2+} increase. However, it is particularly interesting to note that BzATP at this concentration, in contrast with other agonists, causes a large calcium increase which is followed very quickly by a release of fura2 in some cells (Fig. 4). These effects were completely prevented when hepatocytes were pre-incubated for 2h with oATP (300 μM) (Fig. 4B). These observations, in particular the leak of fura2, suggest that P2X7, and possibly P2X4 receptors, could be functional in hepatocytes. Indeed, it is well known that these receptors, particularly P2X7, are able to form a non-selective membrane pore permeable to solutes with molecular masses up to about 800Da [18]. Consequently, we examined the cells for permeability to YO-PRO-1 in the presence of ATP or BzATP.

A typical YO-PRO-1 uptake experiment carried out in spectrofluorometer cuvettes is shown in Fig. 5A. A time-dependent increase in fluorescence intensity was observed in hepatocytes upon BzATP challenge. The increase in YO-PRO-1 accumulation was detected within 10min of agonist application and steady state was reached approximately 30min after the addition of BzATP (Fig. 5A). The dose-response curve obtained after incubation with BzATP for 30min showed an EC_{50} around 450 μM (Fig. 5B). Furthermore, BzATP-stimulated dye uptake was significantly inhibited by the prior incubation of hepatocytes for 2h with

oATP (300 μ M) (Fig. 5B inset). Oxidised ATP did not completely inhibit the YO-PRO-1 uptake induced by BzATP, suggesting that, under these conditions, P2X4 also formed a nonselective membrane pore in hepatocytes, as shown in other cell types [18]. The addition of a very high concentration of ATP (1mM) gave similar results (Fig. 5B and data not shown). This pharmacological behavior is consistent with the agonist profile of P2X7, with BzATP more potent than ATP for activation of this receptor [18].

A unique feature that distinguishes P2X7 receptors from other P2X receptors is their ability to induce changes in cell morphology, cytoskeletal architecture and membrane blebbing [18, 27-28]. Incubation of hepatocytes with BzATP (100 μ M) or ATP (1mM) for 15min triggered membrane blebbing in about 50% of the cells (110/218 cells), (n=3), (Fig. 6). This percentage increased markedly to about 90% (229/256 cells) when hepatocytes were incubated with 300 μ M BzATP, whereas prior incubation with oATP (300 μ M) for 2h almost completely prevented blebbing (12/255 cells). Perfusion of BzATP (300 μ M) or ATP (1mM) for a short period of time (2-3 min) induced membrane blebs, which appeared rapidly in some hepatocytes, and much more slowly in others (Fig. 6B, and Supplementary Mov. 2S). Membrane blebs were fully reversible in almost all hepatocytes (Supplementary Mov. 2S). YO-PRO-1 uptake, also observed over the same time frame, did not correlate with membrane blebbing. As reported for other cell types [18, 27], blebs could appear before or after the detection of YO-PRO-1 fluorescence (Fig. 6).

YO-PRO-1 uptake and membrane blebbing, both of which induced by BzATP and ATP and inhibited by oATP, indicated that P2X7 receptors, and possibly P2X4 receptors, were functional. These two receptors are commonly expressed in the same tissues or cells [1]. However, in our condition, it is very difficult to distinguish the activation of P2X4 from that of P2X7 [18, 25]. Moreover, P2Y receptor expression by hepatocytes complicates the issue even further [10]. Nevertheless, BzATP and high concentrations of ATP induced membrane

blebbing, strongly suggests that P2X7 receptors are functional, as this effect is associated with the activation of P2X7 receptors only [18, 27-28]. The expression of functional P2X7 receptors in hepatocytes could account for the observation that submillimolar concentrations of extracellular ATP induced the death of these cells [12; 29] and open up new fields of investigation, as this receptor has specific properties including cytotoxicity and a role in apoptosis induction.

Including our results, at least five P2 receptors (P2Y1, P2Y2, P2Y4, P2X4 and P2X7) have been identified in hepatocytes. Each of these receptors can increase intracellular Ca^{2+} concentration. Potentially located in different parts of the cell, these receptors would allow fine modulation of the Ca^{2+} signal in time and space which might account for the involvement of ATP in many different situations, such as regulation of cell volume [5], resistance to hypoxia [30], bile secretion [25] and liver regeneration [31].

4. Acknowledgments

E.G. was supported by a Studentship from INSERM (poste d'accueil INSERM), by a Sanofi Prize studentship and by the Groupe Francophone d'Hépatologie Gastro-entérologie et Nutrition Pédiatriques. We thank Julie Sappa and Karen Brunel-Lafargue for their help editing the manuscript, and Josiane Simon for excellent technical assistance.

5. References

- [1] Ralevic, V. and Burnstock, G. (1998) Receptors for purines and pyrimidines. *Pharmacol. Rev.* 50, 413-492.
- [2] Schwiebert, E.M. and Zsembery, A. (2003) Extracellular ATP as a signaling molecule for epithelial cells. *Biochim. Biophys. Acta* 1615, 7-32.
- [3] Feranchak, A.P. and Fitz, J.G. (2002) Adenosine triphosphate release and purinergic regulation of cholangiocyte transport. *Semin. Liver Dis.* 22, 251-262.
- [4] Schlosser, S.F., Burgstahler, A.D. and Nathanson, M.H. (1996) Isolated rat hepatocytes can signal to other hepatocytes and bile duct cells by release of nucleotides. *Proc. Natl. Acad. Sci. USA* 93, 9948-9953.
- [5] Feranchak, A.P., Fitz, J.G. and Roman, R.M. (2000) Volume-sensitive purinergic signaling in human hepatocytes. *J. Hepatol.* 33, 174-182.
- [6] Dranoff, J.A., Masyuk, A.I., Kruglov, E.A., LaRusso, N.F. and Nathanson, M.H. (2001) Polarized expression and function of P2Y ATP receptors in rat bile duct epithelia. *Am. J. Physiol.* 281, G1059-1067.

- [7] Roman, R.M. and Fitz, J.G. (1999) Emerging roles of purinergic signaling in gastrointestinal epithelial secretion and hepatobiliary function. *Gastroenterology* 116, 964-979.
- [8] Takemura, S., Kawada, N., Hirohashi, K., Kinoshita, H. and Inoue, M. (1994) Nucleotide receptors in hepatic stellate cells of the rat. *FEBS Lett.* 354, 53-56.
- [9] Hashimoto, N., Watanabe, T., Shiratori, Y., Ikeda, Y., Kato, H., Han, K., Yamada, H., Toda, G. and Kurokawa, K. (1995) Prostanoid secretion by rat hepatic sinusoidal endothelial cells and its regulation by exogenous adenosine triphosphate. *Hepatology* 21, 1713-1718.
- [10] Schofl, C., Ponczek, M., Mader, T., Waring, M., Benecke, H., von zur Muhlen, A., Mix, H., Cornberg, M., Boker, K.H., Manns, M.P. and Wagner, S. (1999) Regulation of cytosolic free calcium concentration by extracellular nucleotides in human hepatocytes. *Am. J. Physiol.* 276, G164-172.
- [11] Surprenant, A., Rassendren, F., Kawashima, E., North, R.A. and Buell, G. (1996) The cytolytic P2Z receptor for extracellular ATP identified as a P2X receptor (P2X7). *Science* 272, 735-738.
- [12] Zoetewij, J.P., van de Water, B., de Bont, H.J. and Nagelkerke, J.F. (1996) The role of a purinergic P2z receptor in calcium-dependent cell killing of isolated rat hepatocytes by extracellular adenosine triphosphate. *Hepatology* 23, 858-865.

- [13] Capiod, T. (1998) ATP-activated cation currents in single guinea-pig hepatocytes. *J. Physiol.* 507, 795-805.
- [14] Clair, C., Tran, D., Boucherie, S., Claret, M., Tordjmann, T. and Combettes, L. (2003) Hormone receptor gradients supporting directional Ca^{2+} signals: direct evidence in rat hepatocytes. *J. Hepatol.* 39, 489-495.
- [15] Van Rooijen, N., Kors, N., vd Ende, M., and Dijkstra, C.D. (1990) Depletion and repopulation of macrophages in spleen and liver of rat after intravenous treatment with liposome-encapsulated dichloromethylene diphosphonate. *Cell Tissue Res.* 260, 215-22.
- [16] Dijkstra, C.D., Dopp, E.A., Joling, P. and Kraal, G. (1985) The heterogeneity of mononuclear phagocytes in lymphoid organs: distinct macrophage subpopulations in the rat recognized by monoclonal antibodies ED1, ED2 and ED3. *Immunology* 54, 589–599.
- [17] Buell, G., Collo, G. and Rassendren, F. (1996) P2X receptors: an emerging channel family. *Eur. J. Neurosci.* 8, 2221-2228.
- [18] North, R.A. (2002) Molecular physiology of P2X receptors. *Physiol. Rev.* 82, 1013-1067.
- [19] Bowler, J.W., Bailey, R.J., North, R.A. and Surprenant, A. (2003) P2X₄, P2Y₁ and P2Y₂ receptors on rat alveolar macrophages. *Br. J. Pharmacol.* 140, 567-575.

- [20] Xiang, Z., Lv, J., Jiang, P., Chen, C., Jiang, B. and Burnstock, G. (2006) Expression of P2X receptors on immune cells in the rat liver during postnatal development. *Histochem. Cell. Biol.* 126, 453-463.
- [21] Seglen, P.O. (1976) Preparation of isolated rat liver cells. *Methods Cell. Biol.* 13, 29-83.
- [22] Tennesi, L., Gibbons, S.J., and Talamo, B.R. (1998) Expression and trans-synaptic regulation of P2x4 and P2z receptors for extracellular ATP in parotid acinar cells. Effects of parasympathetic denervation. *J. Biol. Chem.* 273, 26799-26808.
- [23] Collo, G., Neidhart, S., Kawashima, E., Kosco-Vilbois, M., North, R.A. and Buell, G. (1997) Tissue distribution of the P2X7 receptor. *Neuropharmacology* 36, 1277-1283.
- [24] Le, K.T., Paquet, M., Nouel, D., Babinski, K. and Seguela, P. (1997) Primary structure and expression of a naturally truncated human P2X ATP receptor subunit from brain and immune system. *FEBS Lett.* 418, 195-199.
- [25] Doctor, R.B., Matzakos, T., McWilliams, R., Johnson, S., Feranchak, A.P. and Fitz, J.G. (2005) Purinergic regulation of cholangiocyte secretion: identification of a novel role for P2X receptors. *Am. J. Physiol.* 288, G779-786.
- [26] Di Virgilio, F. (2003) Novel data point to a broader mechanism of action of oxidized ATP: the P2X7 receptor is not the only target. *Br. J. Pharmacol.* 140, 441-443.

- [27] Virginio, C., MacKenzie, A., North, R.A. and Surprenant, A. (1999) Kinetics of cell lysis, dye uptake and permeability changes in cells expressing the rat P2X7 receptor. *J. Physiol.* 519, 335-334.
- [28] Verhoef, P.A., Estacion, M., Schilling, W. and Dubyak, G.R. (2003) P2X7 receptor-dependent blebbing and the activation of Rho-effector kinases, caspases, and IL-1 beta release. *J. Immunol.* 170, 5728-5738.
- [29] Cui, T.X., Iwai, M., Hamai, M., Minokoshi, Y., Shimazu, T. and Horiuchi, M. (2000) Aggravation of chemically-induced injury in perfused rat liver by extracellular ATP. *Life Sci.* 66, 2593-2601.
- [30] Carini, R., Alchera, E., De Cesaris, M.G., Splendore, R., Piranda, D., Baldanzi, G. and Albano, E. (2006) Purinergic P2Y2 receptors promote hepatocyte resistance to hypoxia. *J. Hepatol.* 45, 236-245.
- [31] Thevananther, S., Sun, H., Li, D., Arjunan, V., Awad, S.S., Wyllie, S., Zimmerman, T.L., Goss, J.A. and Karpen, S.J. (2004) Extracellular ATP activates c-jun N-terminal kinase signaling and cell cycle progression in hepatocytes. *Hepatology* 39, 393-402.

6. Figure legends

Figure 1: Identification of P2X receptor mRNA in isolated hepatocytes.

Rat heart (P2X1, P2X4-5) and brain (P2X2-3, P2X6-7) preparations were used as positive controls, and omission of reverse transcriptase from the reverse transcription mixture as a negative control (-RT). P2X4 and P2X7 mRNAs were detected in each hepatocyte preparation (n=6). The expected sizes of the DNA fragments are detailed in the supplementary data (Tab. 1S).

Figure 2: Expression of P2X4 and P2X7 receptors in isolated hepatocytes.

A: RT-PCR analysis showing similar levels of P2X4 and P2X7 receptor mRNAs in hepatocytes isolated from control (lane 1) and clodronate-treated rats (lane 2).

B: Western blot analysis demonstrating the presence of P2X4 and P2X7 proteins in hepatocytes. For P2X4 detection (left panel), rat salivary gland membrane proteins (lane 1) were run in parallel with hepatocyte lysates from control (lane 2) and clodronate-treated rats (lane 3). P2X7 (right panel) was detected at similar levels in hepatocytes isolated from control (lane 3) and clodronate-treated rats (lane 4). Lysates of P2X7-transfected HEK cells were used as a positive control (lane 2). P2X7 was not detected in wild-type HEK cells (lane 1). Results were confirmed in at least three independent experiments.

Figure 3: Immunolocalization of P2X4 and P2X7 receptors in isolated hepatocytes.

The distribution of the receptors was visualised using FITC-conjugated secondary antibodies. Confocal microscopy: the images correspond to a complete compiled z series of 22 xy sections taken in 0.4 μ m steps.

A: P2X4 was localised at the cell plasma membrane and throughout the cytoplasm. Inset: Confocal analysis showed strong labeling near the bile canaliculus area in hepatocyte doublets. Compilation of 3 z sections taken in 0.3 μ m steps. Bar=10 μ m.

B: Staining with the anti-P2X7 antibody was patchy and restricted to the plasma membrane. Inset: no staining for the P2X7 receptor was detected in the bile canaliculus area. Compilation of 3 z sections taken in 0.3 μ m steps. Bar=10 μ m.

Figure 4: BzATP induced Ca²⁺ increase and release of fura2 in individual hepatocytes.

A: fura-2-loaded hepatocytes were sequentially stimulated with increasing concentrations of BzATP (30 and 300 μ M) for the times indicated by the horizontal bars. Addition of the low dose of BzATP was followed by Ca²⁺ signal similar to InsP3-dependant agonists. After washing, addition of a high concentration of BzATP (300 μ M) induced a rapid and strong increase in Ca²⁺ in all cells, which was followed more or less quickly by a second large Ca²⁺ increase and a release of fura2 (cell a and c in images 3 and 5).

B: Pre-incubation of hepatocytes with oATP (300 μ M) for 2h did not modify the BzATP-induced Ca²⁺ increase but completely prevented both the release of fura2 and the second large Ca²⁺ increase. The traces shown are representative of the Ca²⁺ signal observed in the presence of BzATP in responding cells in 2 independent experiments.

Figure 5: YO-PRO-1 uptake in hepatocytes.

A: Time-course of YO-PRO-1 uptake in isolated hepatocytes, determined as the increase in fluorescence over time. Hepatocytes were incubated in the presence or absence of oATP (300 μ M) for 2h at 37°C. Cells were transferred in spectrofluorometer cuvettes and YO-PRO-1 (1 μ M) was added onto cells at t=0. BzATP (300 μ M) or vehicle was added 3min later (arrow). Triton (T, 0.01%) was added at the end of the experiments to assess the YO-PRO-1 maximum

fluorescence after cell permeabilization. Traces are representative of 5 independent experiments.

B: Dose-response curves for BzATP and ATP-induced YO-PRO-1 uptake.

Suspensions of hepatocytes were added to 96-well plates (50,000cells/well) and incubated for 30min at 37°C with YO-PRO-1 (1μM) and BzATP (■) or ATP (▼). Changes in YO-PRO-1 fluorescence were then monitored in a 96-well plate fluorometer. Values were normalized with respect to the fluorescence measured in cells incubated for the same time in the presence of YO-PRO-1 alone for each experiment (% of control cells).

Inset: Preincubation with oATP (300μM, 2h) significantly reduced the uptake of YO-PRO-1 induced by BzATP (300μM).

The data are means ± SEM for four to eight determinations in three independent experiments.

Figure 6: BzATP and ATP induced the formation of membrane blebs in isolated hepatocytes.

Formation of membrane blebs induced by BzATP (300μM, panel A) or ATP (1mM, panel B), monitored by phase contrast microscopy (left columns). The right columns show YO-PRO-1 uptake for the same cells, as assessed by epifluorescence microscopy. Images were taken at T=0 and 5 and 15 minutes after the addition of agonists

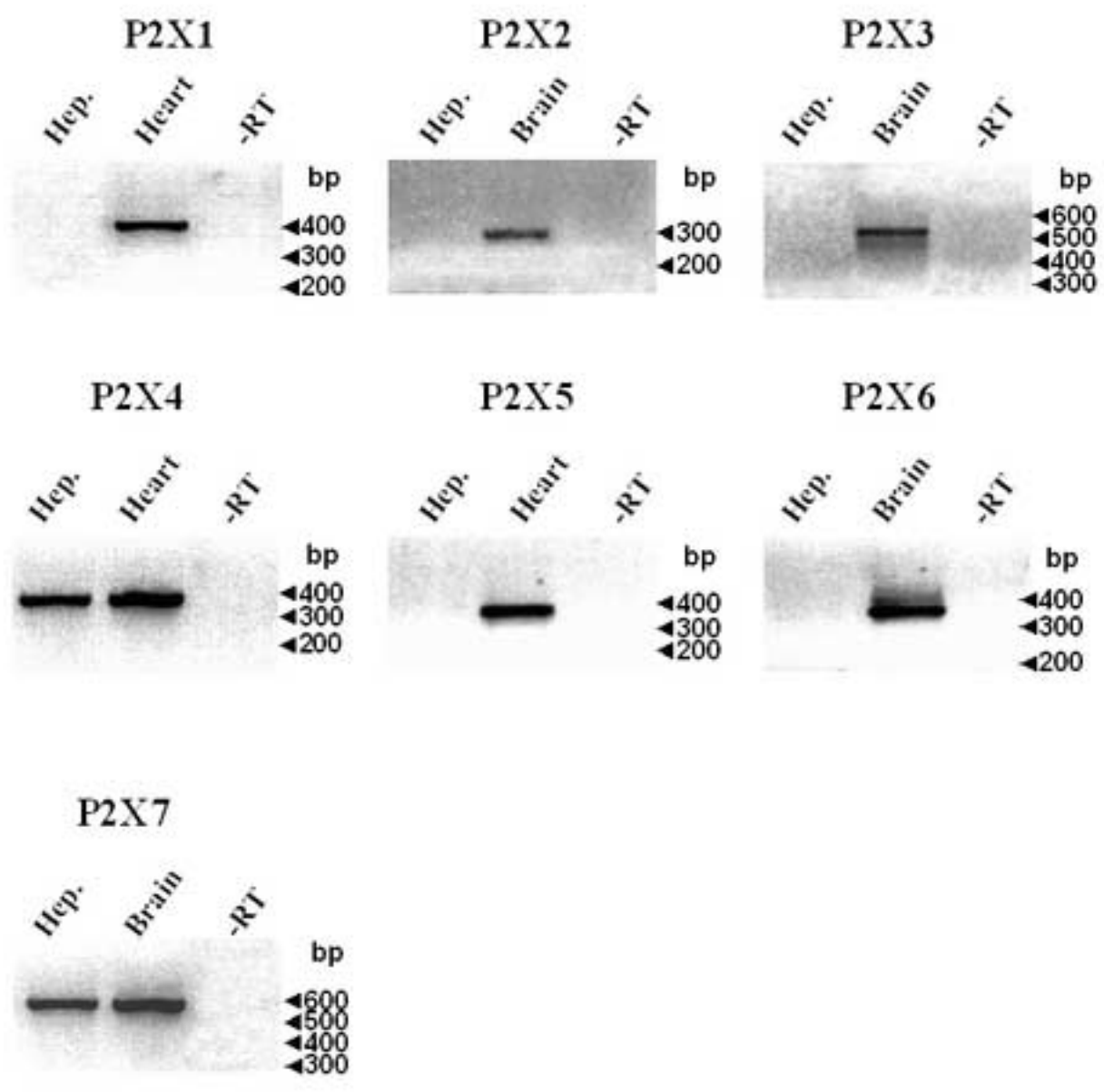


Fig. 1

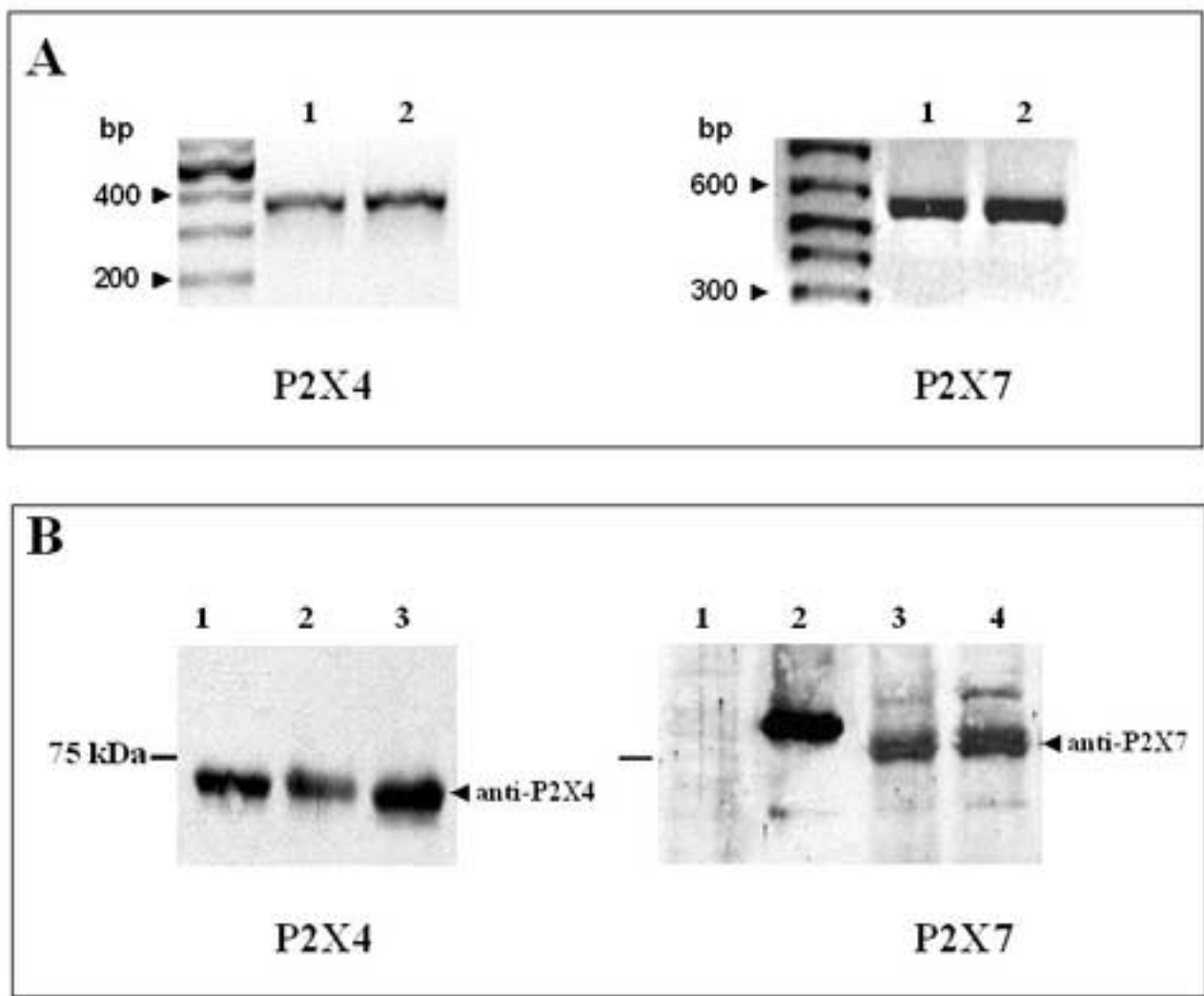


Fig. 2

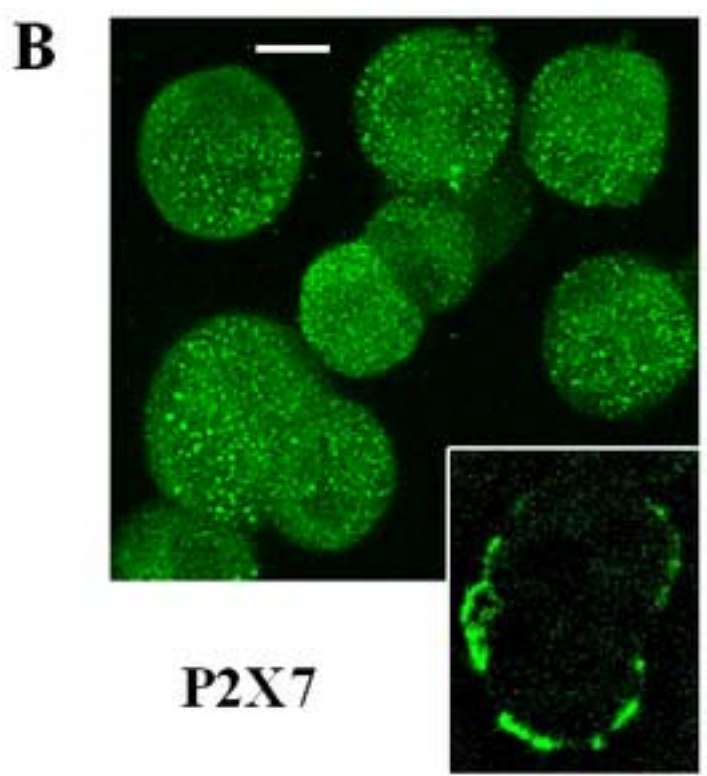
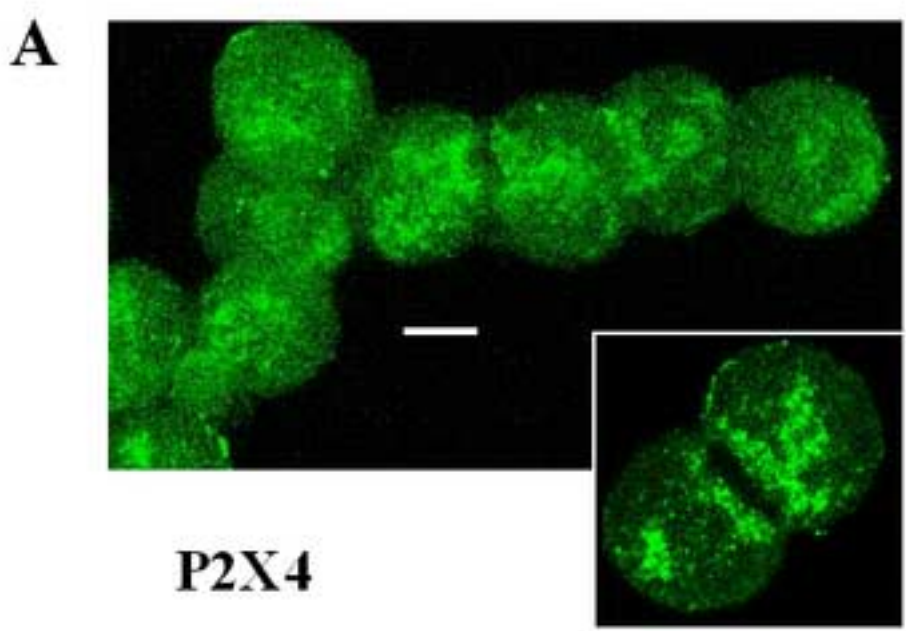


Fig. 3

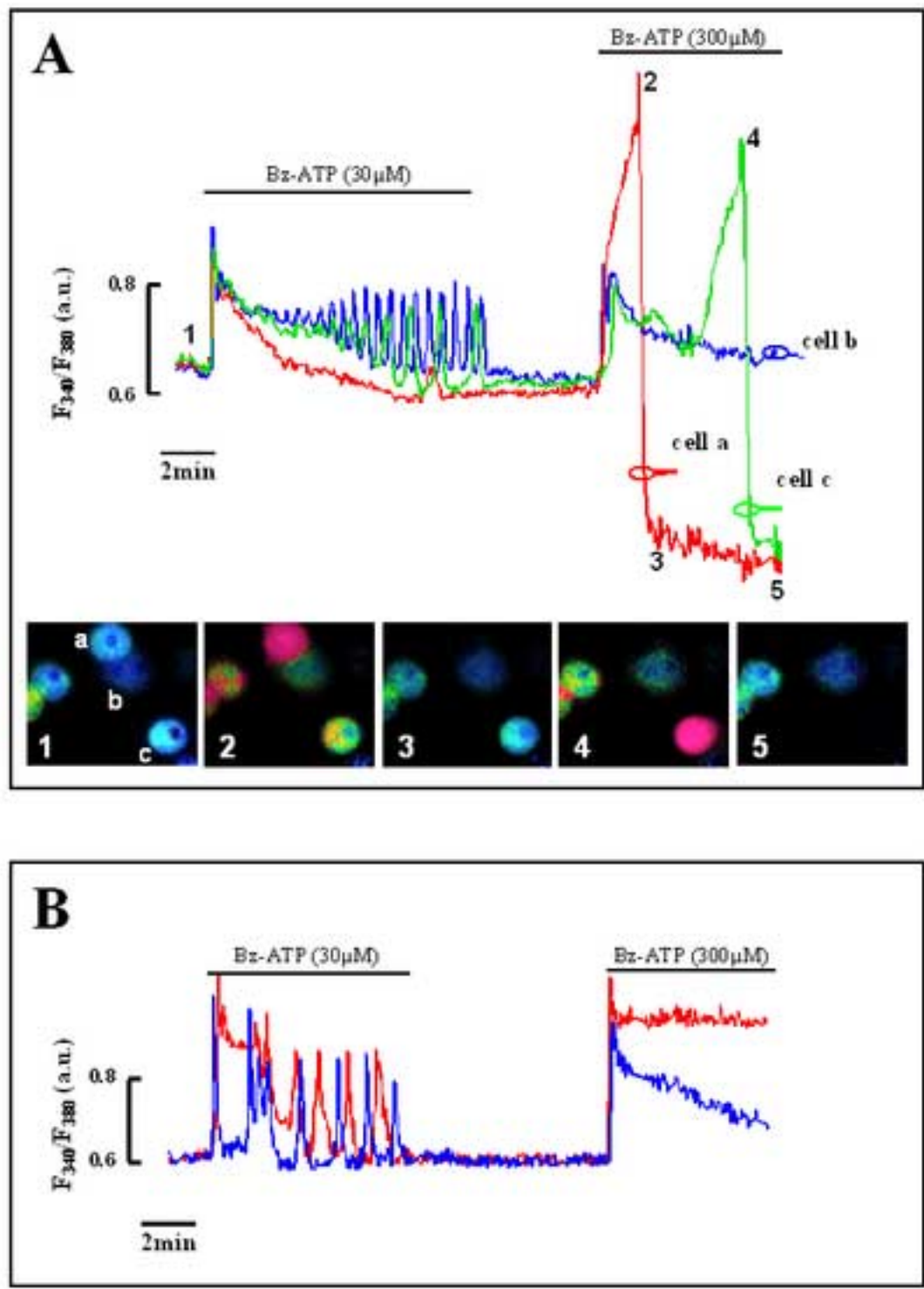


Fig. 4

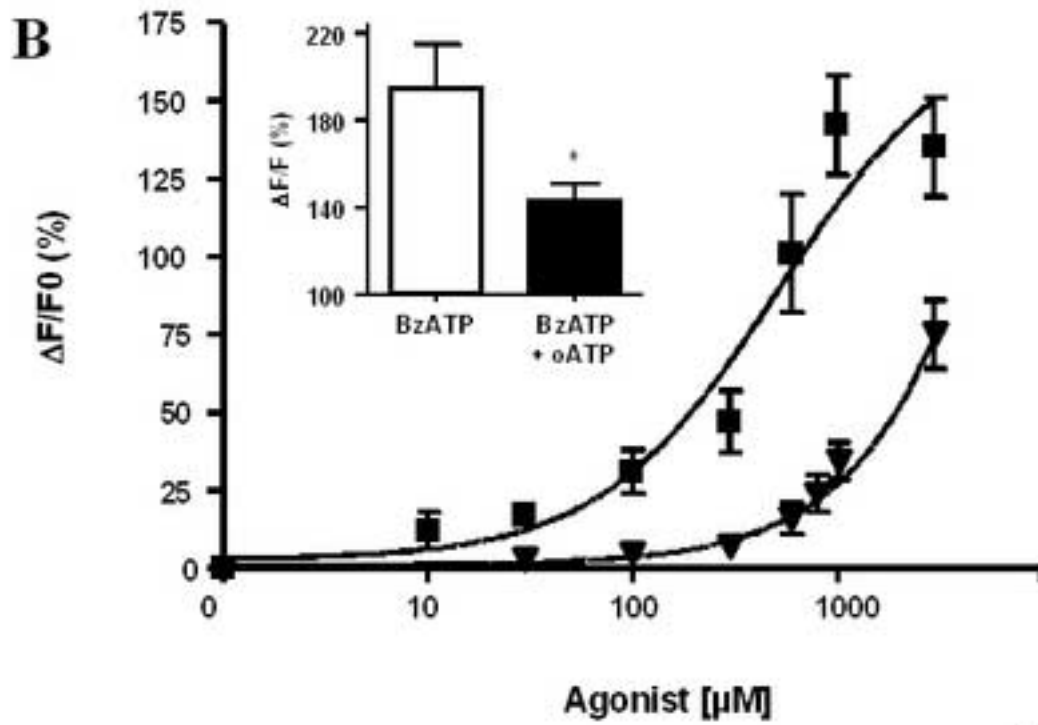
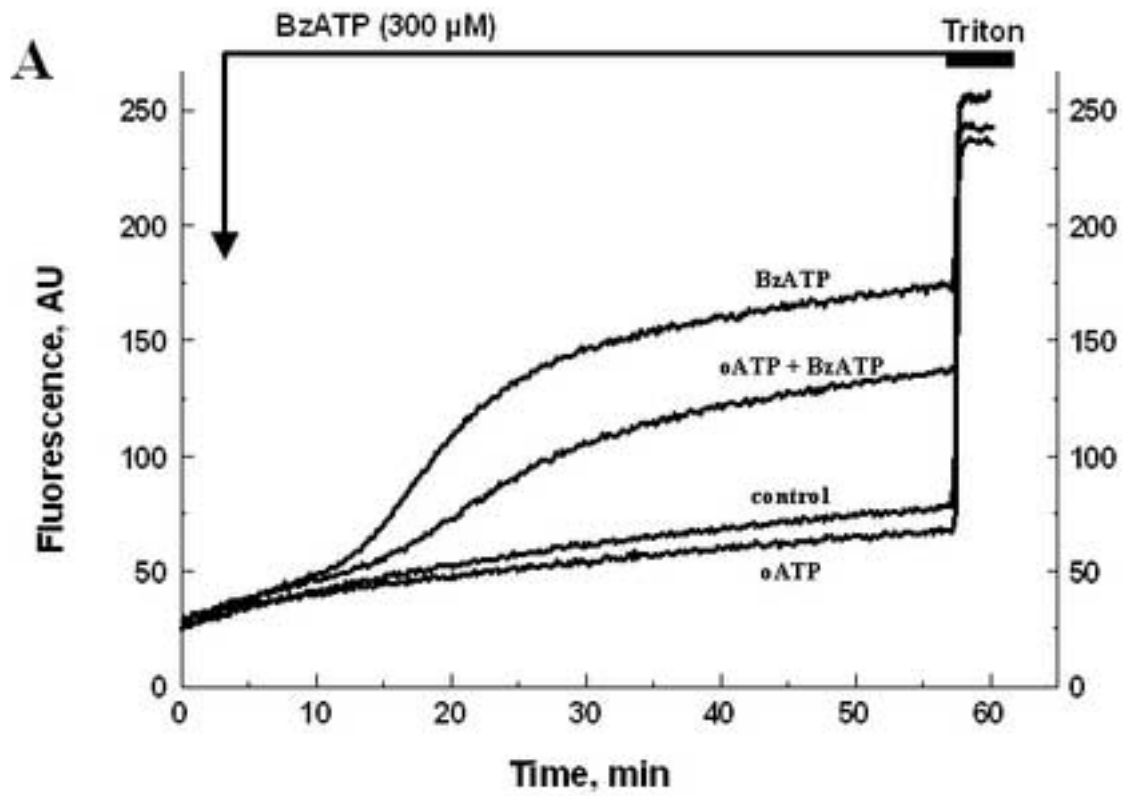


Fig. 5

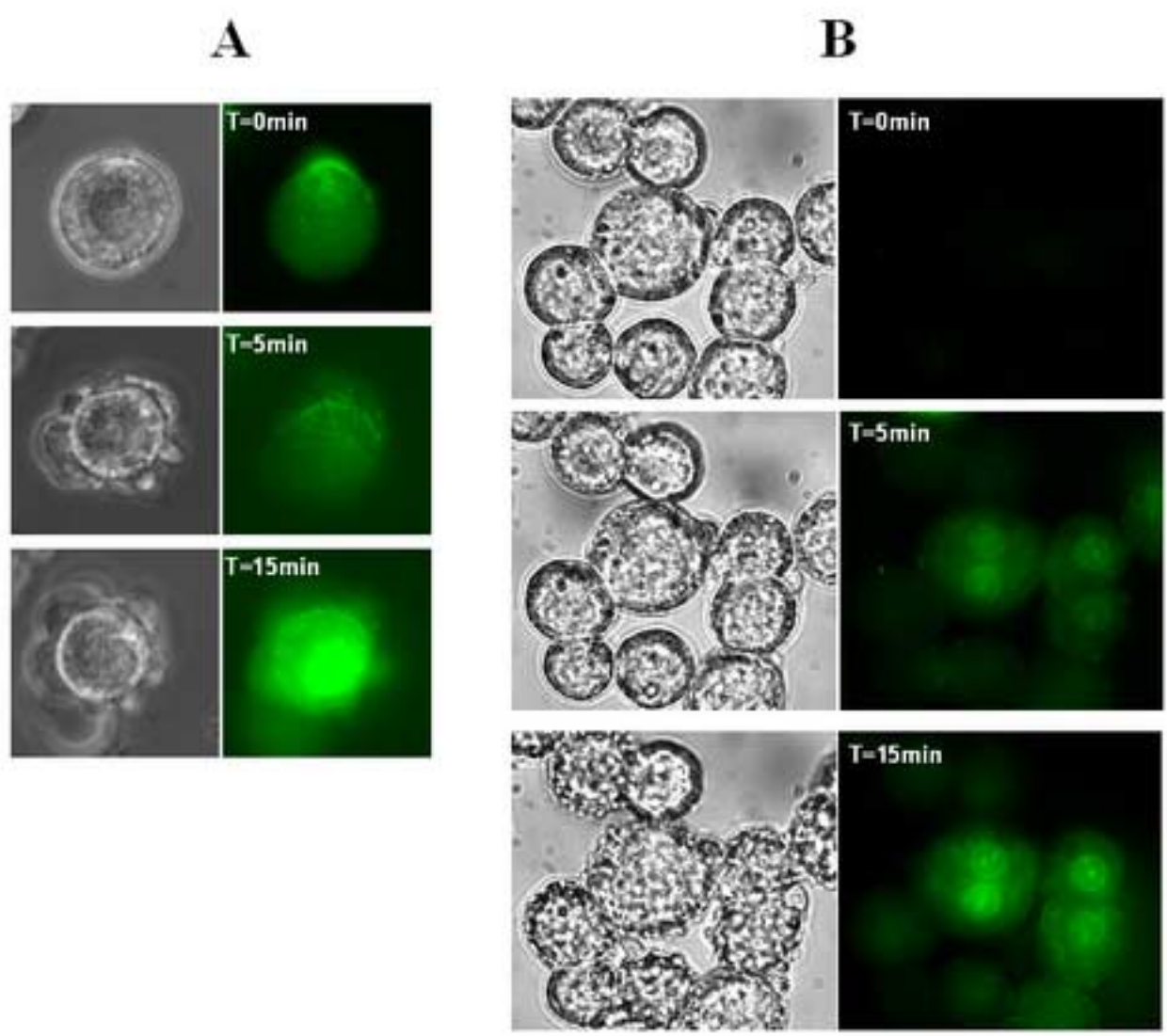


Fig. 6